

solved and controversial question. Selective stimulation of  $\gamma\delta$  T cells by carbohydrates has been suggested (16). Our studies demonstrate that these ligands are phosphorylated metabolites of a thymidine-containing nucleotide conjugate named TUBag4. To our knowledge, thymidine-containing nucleotide conjugates had not been previously reported in nature. They may be involved in a metabolic pathway related to DNA, such as cell proliferation or nucleic acid repair. Such molecules would fit with the "stress antigens" or "conserved primitive stimuli" theoretically expected for  $\gamma\delta$  T lymphocytes (17). Understanding their metabolic function in the producing cell may help to elucidate the physiological role of reactive  $\gamma\delta$  T cells. Our results may also provide clues to understanding autoimmune diseases, for example, T cell help for production of pathogenic immunoglobulin G to DNA in lupus patients frequently involves  $\gamma\delta$  T cells (18), and this may be triggered by TUBags or structurally related stimuli.

## REFERENCES AND NOTES

1. E. M. Janis, S. H. E. Kaufmann, R. H. Schwartz, D. M. Pardoll, *Science* **244**, 713 (1989); R. L. Modlin *et al.*, *Nature* **339**, 544 (1989).
2. R. A. O'Brien *et al.*, *Cell* **57**, 667 (1989); A. Augustin, R. T. Kubo, G. K. Sim, *Nature* **340**, 239 (1989); M. P. Happ, R. T. Kubo, E. Palmer, W. K. Born, R. L. O'Brien, *ibid.* **342**, 696 (1989); W. Born *et al.*, *Science* **249**, 67 (1990); W. Born *et al.*, *Immunol. Today* **11**, 40 (1990).
3. A. Haregewoin, G. Soman, R. C. Horn, R. W. Finberg, *Nature* **340**, 309 (1989); P. Fisch *et al.*, *Science* **250**, 1269 (1990); P. Fisch *et al.*, *J. Immunol.* **148**, 2315 (1992); I. Kaur *et al.*, *ibid.* **150**, 2046 (1993).
4. H. Holoshitz, F. Konig, J. E. Coligan, J. De Bruyn, S. Strober, *Nature* **339**, 226 (1989); D. Kabelitz, A. Bender, S. Schondelmaier, B. Schoel, S. H. E. Kaufmann, *J. Exp. Med.* **171**, 667 (1990).
5. K. Pfeffer, B. Schoel, H. Gulle, S. H. E. Kaufmann, H. Wagner, *Eur. J. Immunol.* **20**, 1175 (1990); K. Pfeffer *et al.*, *J. Immunol.* **148**, 575 (1992).
6. F. Davodeau *et al.*, *J. Immunol.* **151**, 1214 (1993).
7. P. Constant *et al.*, data not shown.
8. The peak detected at 13.0 min in HPAEC analysis of TUBag4 was collected, and its ability to stimulate clone G115 (measured in arbitrary stimulation units) matched that of total TUBag4 before HPAEC separation.
9. Each individual  $^{13}\text{C}$  chemical shift was obtained through its coupling with correlated  $^1\text{H}$  signals during the heteronuclear HMQC and HMBC experiments. The linkage of 2-deoxyribose with thymine was established from HMBC results, as the  $^1\text{H}$   $\delta$  6.280-ppm signal (2-deoxyribose H-1) correlates with a  $^{13}\text{C}$  signal at  $\delta$  136 ppm (thymine C-6), whereas the  $^1\text{H}$   $\delta$  7.677-ppm signal (thymine H-6) correlates with the following  $^{13}\text{C}$  signals:  $\delta$  10.46 ppm (thymine Me-5),  $\delta$  83.81 ppm (2-deoxyribose C-1),  $\delta$  150.4 ppm (thymine C-2), and  $\delta$  165.3 ppm (thymine C-4); P. Constant, M. Gilleron, J. Vercauteren, J.-J. Fournié, unpublished data.
10. E. Breitmaier and W. Voelter, *Carbon-13 NMR Spectroscopy*, (VCH, Weinheim, Federal Republic of Germany, VCH, ed. 3, 1987), pp. 401-414.
11. J. A. McCloskey, in *Basic Principles in Nucleic Acid Chemistry*, P. O. P. Tso, Ed. (Academic Press, New York, 1974), vol: I, chap. 3.
12. Phosphatase reactions were done with either 3 U of calf intestine alkaline phosphatase (Boehringer type 713023) or nucleotide pyrophosphatase from *Crotalus adamanteus* venom (Sigma type II, 0.5 U) incubated in 100  $\mu\text{l}$  of 50 mM tris (pH 8.4) at 37°C for 120 min.
13. Similar HPAEC retention times were found when comparing the biologically active fractions of TUBag1 chromatography with those from venom nucleotide pyrophosphatase-treated TUBag4.
14. P. Constant, Y. Poquet, M. A. Peyrat, M. Bonneville, J.-J. Fournié, unpublished data.
15. D. Kabelitz *et al.*, *J. Exp. Med.* **173**, 1331 (1991).
16. D. H. Raulet, *Nature* **339**, 342 (1989); J. L. Strominger, *Cell* **57**, 895 (1989); W. Haas, P. Pereira, S. Tonegawa, *Annu. Rev. Immunol.* **11**, 637 (1993).
17. C. A. Janeway Jr., B. Jones, A. Hayday, *Immunol. Today* **9**, 73 (1988).
18. S. Rajagopalan, T. Zordan, G. C. Tsokos, S. K. Datta, *Proc. Natl. Acad. Sci. U.S.A.* **87**, 7020 (1990).
19. F. Davodeau *et al.*, *J. Biol. Chem.* **268**, 15455 (1993).
20. The proportion of  $\gamma\delta$  cells after culture without TUBag4 versus with TUBag4 were the following: donor 1, 0.9/69.5; donor 2, 2.6/86.5; donor 3, 5.0/74.1; and donor 4, 1.0/27.2. After culture with TUBag4,  $\gamma\delta$  cells from all donors tested expressed V $\gamma$ 9 and V $\delta$ 2 regions (Fig. 3 C) (21).
21. F. Davodeau, M. A. Peyrat, M. Bonneville, unpublished data.
22. We thank M. A. Laneelle for cultures of *M. tuberculosis* H37Rv; M. Gilleron and J. Vercauteren for NMR experiments; and G. Tuffal R. Albigo, A. Godart, Y. Jacques, M. Daffé, and P. Lerouge for technical advice. This work is part of the doctorat de l'Université Paul Sabatier (P.C.). Supported in part by the World Health Organization and United Nations Development Programme for Vaccine Development (IMMTUB n°92TB0028), l'Association pour la Recherche contre le Cancer (ARC 6690), and institutional grants from the CNRS (Interface Chimie-Biologie) and la Région Midi-Pyrénées (RECH/ 9200841).

2 November 1993; accepted 1 February 1994

## Telomere-Led Premeiotic Chromosome Movement in Fission Yeast

Yuji Chikashige, Da-Qiao Ding, Hironori Funabiki, Tokuko Haraguchi, Shinro Mashiko, Mitsuhiro Yanagida, Yasushi Hiraoka

The movement of chromosomes that precedes meiosis was observed in living cells of fission yeast by fluorescence microscopy. Further analysis by in situ hybridization revealed that the telomeres remain clustered at the leading end of premeiotic chromosome movement, unlike mitotic chromosome movement in which the centromere leads. Once meiotic chromosome segregation starts, however, centromeres resume the leading position in chromosome movement, as they do in mitosis. Although the movement of the telomere first has not been observed before, the clustering of telomeres is reminiscent of the bouquet structure of meiotic-prophase chromosomes observed in higher eukaryotes, which suggests that telomeres perform specific functions required for premeiotic chromosomal events generally in eukaryotes.

The centromere is generally believed to be a unique chromosomal site that leads the chromosome movement. Here we report a situation in which telomeres proceed first in the direction of travel during chromosome movement. We examined the chromosome dynamics during the process of meiosis in living and fixed cells of fission yeast by the use of a computerized fluorescence microscope system with a cooled charge-coupled device (CCD). Our results reveal that telomeres cluster at the leading end of the chromosome movement during premeiotic stages.

In fission yeast *Schizosaccharomyces pombe*, haploid cells of the opposite mating type,  $h^+$  and  $h^-$ , conjugate upon nitrogen starvation and enter the process of meiosis

(zygotic meiosis); alternatively,  $h^+/h^-$  diploid cells can be directly induced to undergo meiosis (azygotic meiosis) (1-3). A characteristic elongated nuclear morphology, generally called horse tail, is observed during a certain period preceding meiotic divisions (Fig. 1) (4). The horse-tail period includes meiotic prophase defined in higher eukaryotes, during which the association and recombination of homologous chromosomes take place (1, 2).

We first examined chromosome dynamics during meiosis in individual living cells. Fission yeast cells were induced to undergo meiosis and stained with a DNA-specific fluorescent dye, Hoechst 33342; meiotic processes in the stained cells were allowed to proceed on a microscope slide (5). In live meiosis, the noticeable movement of nuclei was observed during karyogamy and the horse-tail period. Selected frames of chromosome dynamics in zygotic meiosis are shown for the period of karyogamy (Fig. 2A) and for the horse-tail (Fig. 2B) and meiotic chromosome segregations (Fig.

Y. Chikashige, D.-Q. Ding, T. Haraguchi, S. Mashiko, Y. Hiraoka, Kansai Advanced Research Center, Communications Research Laboratory, 588-2 Iwaoka, Iwaoka-cho, Nishi-ku, Kobe 651-24, Japan. H. Funabiki and M. Yanagida, Department of Biophysics, Faculty of Science, Kyoto University, Kyoto 606, Japan.

2C). The same results of chromosome dynamics were obtained from azygotic meiosis, except for the lack of karyogamy. During karyogamy, two separate nuclei move together along the long axis of the zygote and fuse after several rounds of oscillatory movement (frames at 0 to 20 min in Fig. 2A). Immediately after nuclear fusion, nuclei turn into the horse-tail shape and start the movement (frames at 22 to 28 min in Fig. 2A). During this movement, a specific portion of the nucleus, which can be seen as a bright spot (indicated by an arrow in Fig. 2B), is kept at the leading end of the movement and makes a U-turn at the end of the cell, when U-shaped or J-shaped morphology can be observed (Fig. 2B). The speed of the leading end of the horse-tail movement was about 5  $\mu\text{m}/\text{min}$  along the long axis of the cell. Before the first meiotic division, a horse-tail nucleus stops movement at the center of the cell and then condenses into the spherical shape (frames at 0 to 70 min in Fig. 2C). Shortly after chromosome condensation, the first meiotic division starts (frames at 80 to 120 min in Fig. 2C), and the second meiotic division follows after an interval of 60 min (frames at 180 to 210 min in Fig. 2C). The observations were made at room temperature, 22°C in this example.

With the use of the nuclear morphology observed in live meiosis as a landmark, the spatial arrangement of chromosomes in fixed specimens was examined in relation to

the nuclear movement. The nuclear localization of centromeres and telomeres was determined by fluorescence in situ hybridization to chromosomal DNA (6), with DNA probes of a centromeric repetitive sequence and a telomere-adjacent sequence (7); nuclear DNA was counterstained with 4,6'-diamidino-2-phenylindole (DAPI). The position of the spindle pole body (SPB), a centrosome-equivalent structure in fungi, was determined by indirect immunofluorescence microscopy to serve as a marker of the leading end of nuclear movement (6). It has been shown by electron microscopy that the SPB is located at the leading end of approaching nuclei during karyogamy (8-10).

The position of telomeres and centromeres within horse-tail nuclei is shown in Fig. 3A. Similar to those observed in live meiosis (compare with Fig. 2B), nuclei at this stage have various morphologies: elongated ones migrating along the long axis of the cell (Fig. 3, A to C and F) and U-shaped or J-shaped ones making a turn (Fig. 3, D to F). In any cases of horse-tail nuclei, telomeres were clustered at a single location close to the SPB (Fig. 3, A to F), whereas centromeres were separated from the SPB (Fig. 3, G and H). At the first meiotic division, however, centromeres resumed their proximity to the SPB (Fig. 3J), whereas telomeres became separated from the SPB (Fig. 3I). In the control experiments in mitotic diploid cells, centromeres were clustered at a single locus near the SPB (Fig. 3L) and telomeres were located at several loci separated from the SPB (Fig. 3K) (7).

We also examined the behavior of centromeres and telomeres during karyogamy. For the entire process of karyogamy, telomeres were clustered near the SPB located

at the leading end of approaching nuclei (Fig. 4, A to D), whereas centromeres were clustered at a location separated from the SPB (Fig. 4E). Two sets of the SPB and the telomere cluster in the approaching nuclei are shown in Fig. 4, A and B. One fused SPB with two separate clusters of telomeres at the middle of the dumbbell-shaped nucleus can be seen in another example (Fig. 4C). A single cluster of telomeres (Fig. 4D) represents the association of homologous sets of telomeres. Thus, the association of homologous telomeres is completed as early as the end of karyogamy. This finding is consistent with the result that only one signal for telomeres was observed in all cases of at least 200 horse-tail nuclei examined (Fig. 3, A to F). On the other hand, one or two signals for centromeres were observed in a horse-tail nucleus (Fig. 3, G and H, and Fig. 4, F and G). We presume that one spot and two spots of centromeres represent the paired and unpaired state of homologous sets of centromere clusters, respectively. The behavior of centromeres, telomeres, and the SPB is summarized in a schematic diagram in Fig. 5.

We have demonstrated premeiotic chromosome movement revealed by DNA-specific vital staining in fluorescence microscopy. Previous observations of fixed specimens by light and electron microscopy have documented that nuclei at the premeiotic stage are heterogeneous in their shape and position within a cell (8-10). Our observations in living specimens clearly indicated that different morphology simply reflects transitional stages of a single moving nucleus. Electron microscopy studies have shown that a bundle of microtubules is located along the horse-tail nucleus with the SPB at

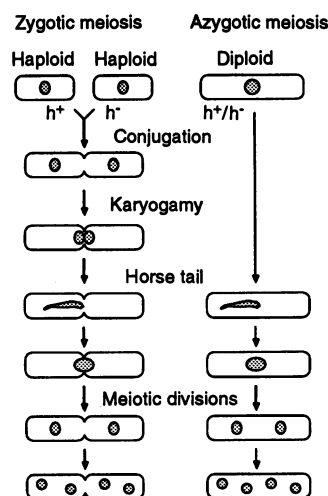


**Fig. 1.** Premeiotic and meiotic processes in fission yeast. From nuclear morphology alone, the horse-tail period cannot be classified into the meiotic stages cytologically defined in higher eukaryotes (16-18). In this report, to distinguish from the subsequent period of meiotic chromosome segregation, we include karyogamy and the horse-tail period within the premeiotic stage, although the horse-tail period includes not only premeiotic interphase but also meiotic prophase defined in higher eukaryotes (1, 2, 8).

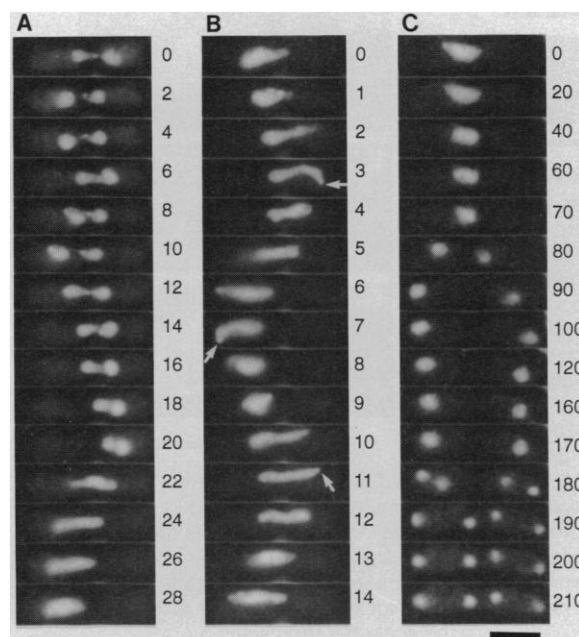


**Fig. 2.** Chromosome dynamics observed in live meiosis. Selected frames of chromosome dynamics during (A) karyogamy, (B) horse-tail, and (C) meiotic chromosome segregations in three independent sets of experiments. Each column is a time-lapse series obtained from a single cell. The numbers at the right side of each column are time in minutes. The scale bar represents 5  $\mu\text{m}$ .

one end of the nucleus (8–10). Immunofluorescence microscopy has also shown that an aster of microtubules radiates from the SPB in the horse-tail stage (11). In addition, the chromosome movement in karyogamy and the horse-tail period was inhibited by the addition of thiabendazole, an inhibitor of microtubule polymerization (12). These observations suggest that the chromosome movement during karyogamy and the horse-tail stage is led by the SPB migrating on an array of microtubules.

Our results show that drastic nuclear reorganization switching the leading position in chromosome movement takes place during the process of meiosis. In a prelude to meiosis, telomeres lead in chromosome movement; once meiotic chromosome segregation starts, however, centromeres lead chromosome movement as they do in mitosis. These telomere dynamics contrast with a generally believed picture that centromeres

are kept engaged with the SPB throughout the life cycle in fission yeast (7). Because telomeres lead in chromosome movement only during the karyogamy and horse-tail stages, telomeres may function specifically in premeiotic chromosomal events such as the association and recombination of homologous chromosomes.

The clustering of telomeres is reminiscent of the bouquet structure of meiotic chromosomes observed in a wide range of animals and plants [reviewed in (13–18)]; chromosomes are kept bundled at the telomere to form the bouquet-like arrangement in meiotic prophase, during which the interlocking of chromosomes disappears and the pairing of homologous chromosomes is completed (16–18). The chromosome movement preceded by telomeres has not been demonstrated before. However, there is an implication in old literatures

that meiotic telomeres are clustered near the centrosome, for example, in mantis (19), suggesting that our findings may be general in eukaryotes [reviewed in (17, 18)]. Why the telomere proceeds first in these chromosome movements is unknown, but it is tempting to speculate that the linearly aligned configuration of chromosomes pulled by telomeres may facilitate the pairing of homologous chromosomes by shuffling and resolving interlocked chromosomes. These studies provide a new way of screening and characterizing mutants from a dynamic aspect. Thus, combined with

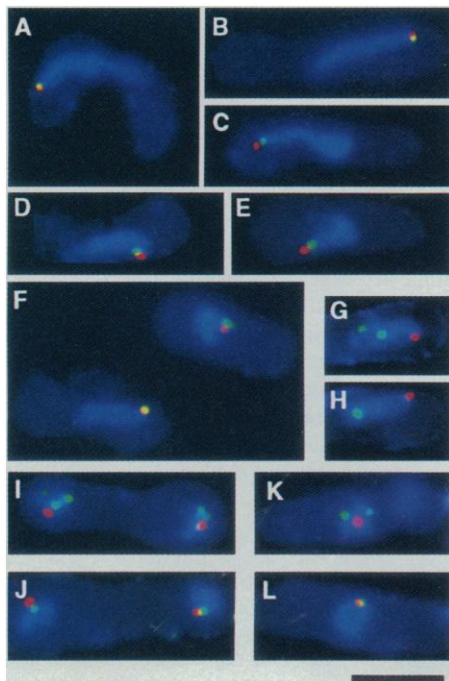


**Fig. 3.** Position of centromeres and telomeres relative to the SPB. Whereas red spots represent the SPB in all cases, green spots represent hybridization signals for either telomeres or centromeres. Some spots appear yellow when a green spot of telomeres overlaps a red spot of the SPB. Whole cells are displayed in which the nuclear region is brightly stained in blue on a faint background of cytoplasm. (A to H) Horse-tail stage; (A to C) telomeres in zygotic horse tail and (D to F) in azygotic horse tail; (G and H) centromeres in azygotic horse tail. (I and J) First meiotic division; (I) telomeres and (J) centromeres. (K and L) Diploid mitosis; (K) telomeres and (L) centromeres. The number of fluorescent signals was examined in a three-dimensional data set, although a single focal plane containing all signals is displayed in the figure for a more simple view. The scale bar represents 5  $\mu$ m.

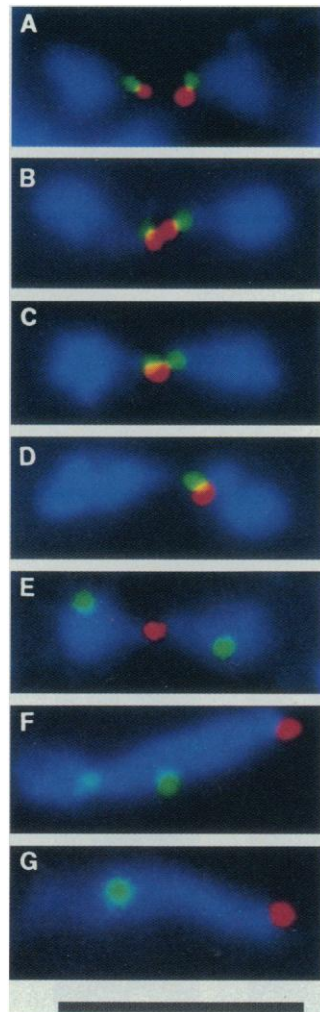


**Fig. 4.** Pairing of homologous telomeres and centromeres: (A to E) karyogamy and (F and G) horse-tail stage. Green spots represent hybridization signals for (A to D) telomeres or (E to G) centromeres, while red spots represent the SPB. Nuclear chromatin is displayed in blue. The scale bar represents 5  $\mu$ m.

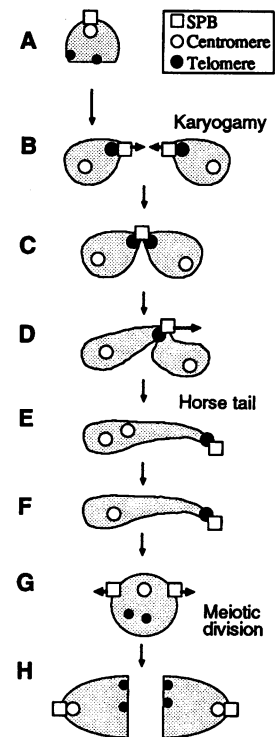


**Fig. 5.** Behavior of telomeres and centromeres. Shaded areas represent nuclear chromatin. At the time of induction to meiosis, telomeres are located at several loci separated from the SPB, while centromeres form a single cluster near the SPB (A). During karyogamy when parental nuclei approach each other, telomeres form a single cluster close to the SPB and centromeres are separated from the SPB (B). The association of homologous chromosomes begins at the telomeres led by the SPB during karyogamy (C and D). Chromosomes have the polarized telomere-centromere configuration with the orientation opposite each other in parental nuclei. After several rounds of oscillation, parental sets of chromosomes are suddenly pulled by the SPB moving to one direction and turn into the horse-tail shape (D and E). By this motion, parental sets of chromosomes now have the same orientation of the polarized telomere-centromere configuration in a horse-tail nucleus. Homologous centromeres become paired at a later stage (F). The proximity of centromeres to the SPB is resumed before or during the first meiotic division (G and H).

genetic approaches, such studies will lead to an understanding of molecular mechanisms for meiotic chromosomal events.

## REFERENCES AND NOTES

- R. Egel, *Mol. Gen. Genet.* **121**, 277 (1973).
- \_\_\_\_\_ and M. Egel-Mitani, *Exp. Cell Res.* **88**, 127 (1974).
- S. Moreno, A. Klar, P. Nurse, *Methods Enzymol.* **194**, 793 (1990).
- C. F. Robinow, *Genetics* **87**, 491 (1977).
- Cells of a homothallic strain of *S. pombe*, h<sup>90</sup> ade6-M210, cultured to mid-log phase in EMM2 (3) containing adenine sulfate (100 µg/ml) were transferred to EMM2 without nitrogen (EMM2-N) and incubated at 26°C to induce conjugation and meiosis. Live meiosis was first observed 6 hours after the nitrogen starvation. Cells were stained with Hoechst 33342 (0.5 µg/ml) in distilled water for 15 min at room temperature and then resuspended in EMM2-N. Live images of Hoechst 33342-stained cells were obtained on a cooled CCD with an exposure of 0.1 to 0.2 s under ultraviolet illumination of a mercury arc lamp. Stained cells were monitored after data collection to verify that spores were formed normally. An Olympus 60 ×/NA1.4 oil-immersion objective lens and a high-selectivity DAPI-Hoechst filter combination (Omega Optical, Brattleboro, VT, and Chroma Technology, Brattleboro, VT) were used in live analysis. The computer-controlled CCD microscope system is based on an Olympus inverted IMT-2 microscope equipped with a Peltier-cooled CCD (Photometrics, Tucson, AZ) with a 1340 by 1037 pixel CCD chip [Kodak KAF1400 (Rochester, NY)]. Details of the microscope system setup are the same as in (20) except that the MicroVAX (Digital Equipment, Boston, MA) was replaced by the Personal Iris 4D/35TG (Silicon Graphics, Mountain View, CA).
- Haploid cells of h<sup>90</sup> ade6-M210 were used for zygotic meiosis, and h<sup>+</sup>/h<sup>-</sup> ade6-M216/ade6-M210 diploid cells were used for azygotic meiosis. Cells were fixed with 3% formaldehyde (freshly prepared from paraformaldehyde) and 0.2% glutaraldehyde in PEM buffer [100 mM Pipes (pH 6.9), 1 mM EGTA, 1 mM MgCl<sub>2</sub>] for 15 min at 26°C. After fixation, cells were permeabilized and treated with ribonuclease A as described (7, 21). The position of the SPB was determined by indirect immunofluorescence microscopy with an antibody to the fission yeast *Sad1* gene product, which is well characterized as a marker of the SPB in fission yeast mitotic cells (7), and a fluorescein-conjugated second antibody. Immunofluorescence labeling was carried out in PEM buffer as described in (22). After immunofluorescence labeling, cells were refixed with 3% formaldehyde and subjected to *in situ* hybridization. Plasmid pRS140 and cosmid cos212 were used as hybridization probes for centromeres and telomeres, respectively; pRS140 hybridizes to centromeric repeats in all three chromosomes (23), and cos212 hybridizes to both ends of chromosome I and II but not to chromosome III (7). DNA fragments were labeled with digoxigenin-dUTP by a terminal transferase reaction with the oligonucleotide tailing kit (Boehringer Mannheim, Indianapolis, IN). The heat-denatured DNA probe was hybridized to chromosomal DNA that had been denatured in 0.1 M NaOH. Hybridization was carried out in 50% formamide and 2× standard saline citrate at 37°C for 12 to 16 hours as described in (21). Hybridization signals were detected with the use of rhodamine-conjugated anti-digoxigenin antibody. Nuclear DNA was counterstained with DAPI (1 µg/ml). Triple-color fluorescent images of DAPI, fluorescein, and rhodamine were obtained on the computerized CCD microscope with an Olympus 100 ×/NA1.3 oil-immersion objective lens, high-selectivity filter combination and a triple-wavelength dichroic mirror (Omega Optical and Chroma Technology) (20).
- H. Funabiki, I. Hagan, S. Uzawa, M. Yanagida, *J. Cell Biol.* **121**, 961 (1993).
- L. W. Olson, U. Eden, M. Egel-Mitani, R. Egel, *Hereditas* **89**, 189 (1978).
- A. Hirata and K. Tanaka, *J. Gen. Appl. Microbiol.* **28**, 263 (1982).
- J. Bähler, T. Wyler, J. Loidl, J. Kohli, *J. Cell Biol.* **121**, 241 (1993).
- I. Hagan and M. Yanagida, unpublished data.
- D.-Q. Ding and Y. Chikashige, unpublished data.
- E. H. Blackburn and J. W. Szostak, *Annu. Rev. Biochem.* **53**, 163 (1984).
- M. P. Maguire, *J. Theor. Biol.* **106**, 605 (1984).
- A. J. Hilliker and R. Appels, *Exp. Cell Res.* **185**, 297 (1989).
- E. Therman and M. Susman, in *Human Chromosomes* (Springer-Verlag, New York, 1992), pp. 165–189.
- B. John, *Meiosis* (Cambridge Univ. Press, Cambridge, 1990).
- C. P. Fussell, in *Meiosis*, P. B. Moens, Ed. (Academic Press, Orlando, FL, 1987), pp. 275–299.
- S. Hughes-Schrader, *Biol. Bull. Woods Hole, Mass.* **85**, 165 (1943).
- Y. Hiraoka, J. R. Swedlow, M. R. Paddy, D. A. Agard, J. W. Sedat, *Semin. Cell Biol.* **2**, 153 (1991).
- S. Uzawa and M. Yanagida, *J. Cell Sci.* **101**, 267 (1992).
- I. M. Hagan and J. S. Hyams, *ibid.* **89**, 343 (1988).
- Y. Chikashige *et al.*, *Cell* **57**, 739 (1989).
- We thank J. W. Sedat, D. A. Agard, H. Chen, M. Jones, M. C. Rykowski, J. S. Minden, and Olympus Optical for their help in constructing our microscope system; E. H. Blackburn and P. Nurse for critical reading of the manuscript; and M. Kotaki for his administrative efforts in opening up this laboratory. Supported by grants from the Japanese Ministry of Posts and Telecommunications; the Science and Technology Agency of Japan (Y.H.); and the Japanese Ministry of Education, Science and Culture [Specially Promoted Research Grant (M.Y.)].

13 December 1993; accepted 17 February 1994

## Requirement for the Yeast Gene *LON* in Intramitochondrial Proteolysis and Maintenance of Respiration

Carolyn K. Suzuki,\* Kitaru Suda, Nan Wang, Gottfried Schatz

The role of protein degradation in mitochondrial homeostasis was explored by cloning of a gene from *Saccharomyces cerevisiae* that encodes a protein resembling the adenosine triphosphate (ATP)-dependent bacterial protease Lon. The predicted yeast protein has a typical mitochondrial matrix-targeting sequence at its amino terminus. Yeast cells lacking a functional *LON* gene contained a nonfunctional mitochondrial genome, were respiratory-deficient, and lacked an ATP-dependent proteolytic activity present in the mitochondria of *Lon*<sup>+</sup> cells. *Lon*<sup>-</sup> cells were also impaired in their ability to catalyze the energy-dependent degradation of several mitochondrial matrix proteins and they accumulated electron-dense inclusions in their mitochondrial matrix.

The turnover of proteins within mitochondria remains poorly understood. Early work suggested that all mitochondrial proteins are degraded at the same rate (1), but later studies have shown that different mitochondrial proteins have different half-lives (2). As mitochondria appear to have evolved from endosymbiotic bacteria, selective degradation of mitochondrial proteins may be mediated by proteases similar to those of present-day bacteria. Indeed, Goldberg, Kužela, and their colleagues have found that the mitochondrial matrix contains an ATP-dependent protease resembling the Lon protease of bacteria (3, 4). Bacterial Lon plays an important role in the controlled degradation of short-lived or abnormal proteins (5).

To assess the physiological importance of the ATP-dependent mitochondrial protease, we sought to clone a *LON* gene

homolog from *Saccharomyces cerevisiae*. We designed degenerate oligonucleotide primers (Fig. 1, arrows), exploiting the sequence conservation between different bacterial Lon proteases and the recently identified Lon homolog from humans (6). Using these primers in the polymerase chain reaction (PCR), we amplified a 1.2-kb fragment from both genomic yeast DNA and from a yeast complementary DNA (cDNA) library (7). The partial sequence of this fragment indicated that the potential protein product was markedly similar to the human and bacterial Lon proteins. This 1.2-kb fragment was used to clone the full-length gene from a yeast cDNA library (8). This gene, which we have designated *LON*, contains an open reading frame encoding a protein of 1133 amino acids.

The sequence of the yeast Lon protein is ~60% similar to the Lon proteases from *Bacillus brevis*, *Myxococcus xanthus*, and *Escherichia coli* and 65% similar to the human Lon homolog. Two regions are highly conserved among all homologs: the putative ATP-binding motifs between amino acids 633 and 730, and the region surround-

C. K. Suzuki, K. Suda, G. Schatz, Biozentrum der Universität Basel, CH-4056 Basel, Switzerland.  
N. Wang, Laboratory of Cell Biology, National Cancer Institute, National Institutes of Health, Bethesda, MD 20892, USA.

\*To whom correspondence should be addressed.